Frequency Stability of Isolated Hydropower Plant with Surge Tank under Different Turbine Control Modes

Weijia Yang[a,b,*] , Jiandong Yang[a], Wencheng Guo[a], Per Norrlund[b,c]

[a] The State Key Laboratory of Water Resources and Hydropower Engineering Science, Wuhan University, Wuhan, 430072, China

[b] Department of Engineering Sciences, Uppsala University, Uppsala, SE-751 21, Sweden

[c] Vattenfall R&D, Älvkarleby, SE-814 26, Sweden

Abstract. Nowadays the Thoma criterion is often violated to diminish the cross section of surge tank, therefore the surge fluctuation is aggravated and frequency stability becomes more deteriorative. The focus of this paper is on stabilizing the low frequency oscillation of an isolated Hydropower plant (HPP) caused by surge fluctuation. From a new perspective of HPP operation mode, frequency stability under power control is investigated and compared with frequency control, by adopting the Hurwitz criterion and numerical simulation. In a theoretical derivation, the governor equations of frequency control and power control are introduced to the mathematical model. For numerical simulation, a governor model with control mode switch-over function is built. The frequency oscillations under frequency control, power control and control mode switch-over are simulated and investigated respectively, with different governor parameters and operation cases. The result shows that the power control has a better performance on frequency stability at the expense of rapidity, comparing with the

frequency control. Other recommendations regarding worst operation cases and choice of control modes are also developed.

Key words: frequency stability; isolated hydropower plant; control mode; operation case; Hurwitz criterion

1 Introduction

Frequency stability refers to the ability of a power system to maintain steady frequency following a severe system upset resulting in a significant imbalance between generation and load [1]. Hydroelectric generating units will undertake the peak modulation and frequency modulation in a power system, hence their frequency stability have been a critical factor of the power system security and power quality.

Especially for the hydropower plant (HPP) with surge tank, with the scale getting larger nowadays, the Thoma criterion [2, 3] is often violated to diminish the cross section of surge tank. Therefore, the surge fluctuation is aggravated and frequency stability becomes more deteriorative [4]. In this case, not only frequency, but also opening and power output would oscillate with the surge fluctuation, therefore frequency stability is actually a typical indicator of the whole system stability. Recently, some huge Chinese HPPs encountered this instability problem during the commissioning, measurements under a load step disturbance are shown in Figure 1. Hence, the focus of this paper is on stabilizing the low frequency oscillation of an

isolated HPP caused by surge fluctuation. If stability cannot be achieved well by standard frequency control (speed control), is power control (power output control) an effective alternative? This question is urgently in need of research.

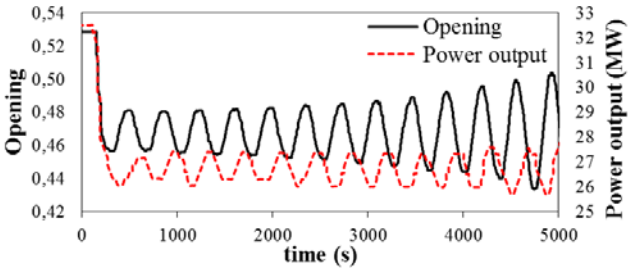

Figure 1. Measurement of oscillations under a load step disturbance from a Chinese HPP

There are several researches on governing system stability of HPP which mainly adopt theoretical derivation [4-6]. However, the mathematical models only take into account equations of ideal governor, so the practical governor control modes are simplified. Moreover, the single theoretical analysis inevitably ignores the water elasticity and nonlinear characteristic of turbine and piping system. There are other simulations and studies on isolated HPP control [7] and influence factors of frequency stability and quality: surge tanks [5, 8], governor setting [9-11], hydraulic system layout [12], power system stabilizer [13, 14] and water column elasticity [15]. Oscillation behavior under frequency control in a pumped-storage HPP is simulated and investigated, the influence of governor parameters (the droop settings, derivative term, dead-band) are discussed [16]. Low frequency oscillation under different frequency control modes are contrasted under islanded operation in [17], and it is found that feed forward controllers should not be used, since they adversely influence the frequency stability. To the best of the author’s knowledge, the water way system in many

numerical models is relatively simplified. What's more, existing studies seldom discuss the frequency stability from the angle of operation mode, such as different control modes and operation cases. In particular, the stability under power control is not well-studied yet.

In this study, frequency stability under power control is investigated and compared with frequency control, from a new perspective of HPP operation mode. Section 2 presents two mathematical models, which are built in this study, for theoretical derivation and numerical simulation respectively. In section 3, by means of theoretical derivation, stability conditions under two control modes are contrasted through adopting Hurwitz criterion. In section 4, the frequency oscillation under frequency control, power control and control mode switch-over are simulated and investigated respectively, with different governor parameters and operation cases.

2 Mathematical model

This study is conducted by both theoretical derivation and simulation, with building two mathematical models respectively. The models are unique in the sense that: in theoretical derivation, the governor equations of frequency control and power control are introduced to the mathematical model; for numerical simulation, a governor model with control mode switch-over function is build. These two models and their main difference are illustrated in this section.

2.1 Model for theoretical derivation

The theoretical derivation of this paper is based on assumptions below: (1) Rigid water hammer is adopted in draw water tunnel with neglecting the elasticity of water and pipe wall. (2) Characteristic of penstock is ignored. (3) Head loss at the bottom of surge tank is not considered. (4) Steady-state characteristic of hydraulic turbine is described by transmission coefficient. (5) Nonlinear characteristic of governor (saturation, rate limiting and dead zone) is ignored. (6) Generator equation is first-order for describing isolated operation. On the basis of assumptions above, the model of water diversion and power generation system is linearized, the basic equations are indicated in Eqs. (1-7), and a schematic diagram is shown in Figure 2.

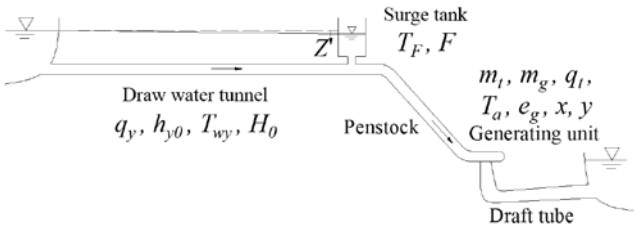

Figure 2. Water way and power generation system in a HPP with surge tank

Dynamic equation of draw water tunnel:

$$z - \frac{2h_{y0}}{H_0} q_y = T_{wy} \frac{\mathrm{d}q_y}{\mathrm{d}t} \tag{1}$$

Continuity equation of surge tank:

$$q_y = q_t - T_F \frac{\mathrm{d}z}{\mathrm{d}t} \tag{2}$$

Moment equation and discharge equation of hydraulic turbine:

$$m_t = -e_h z + e_x x + e_y y \tag{3}$$

$$q_t = -e_{qh} z + e_{qx} x + e_{qy} y \tag{4}$$

Generator equation:

$$T_a \frac{\mathrm{d}x}{\mathrm{d}t} = m_t - (m_g + e_g x) \tag{5}$$

Governor equations:

Frequency control (speed control):

$$(T_y + b_p K_P T_y)\frac{\mathrm{d}^2 y}{\mathrm{d}t^2} + (1 + b_p K_P + b_p K_I T_y)\frac{\mathrm{d}y}{\mathrm{d}t} + b_p K_I y = -(K_P \frac{\mathrm{d}x}{\mathrm{d}t} + K_I x) \tag{6}$$

Power control (power output control):

$$T_y \frac{\mathrm{d}^2 y}{\mathrm{d}t^2} + \frac{\mathrm{d}y}{\mathrm{d}t} = \frac{\mathrm{d}p_g}{\mathrm{d}t} + e_p K_I (p_g - p_t) \tag{7}$$

The details of the symbols in the equations above are given in Appendix A. These two control modes correspond to the function of the governor in section 2.2, more descriptions are presented later. It is worth noting that, in this study, the characteristic coefficient of power grid load (e_g) is set to 0, which represents the resistive constant-power load for achieving a conservative and robust solution [20].

2.2 Model for numerical simulation

The modeling described in this section is based on the software TOPSYS [18], which is developed for analyzing transient processes of HPP based on VC++. Comparing with the assumptions of theoretical derivation above, the model has these improvements: (1) Elastic water hammer is adopted in draw water tunnel considering the elasticity of water and pipe wall. (2) Characteristic of penstock is taken into account. (3) Head loss at the bottom of surge tank is considered. (4) Characteristic curve of hydraulic turbine is introduced. The generator equation is still first-order for simulating isolated operation.

The turbine control subsystem in TOPSYS is improved to simulate different control

modes and their switch-over. The control mode switch-over is implemented by a combined control system in a parallel structure. Each control mode can be assigned to a separate controller. However, the controllers all actuate the same main servo-positioner to control the opening. The power controller command signal still follows the actual power output signal in the frequency control mode [19], and vice versa. Then the bump-free switch-over between frequency control and power control can be achieved.

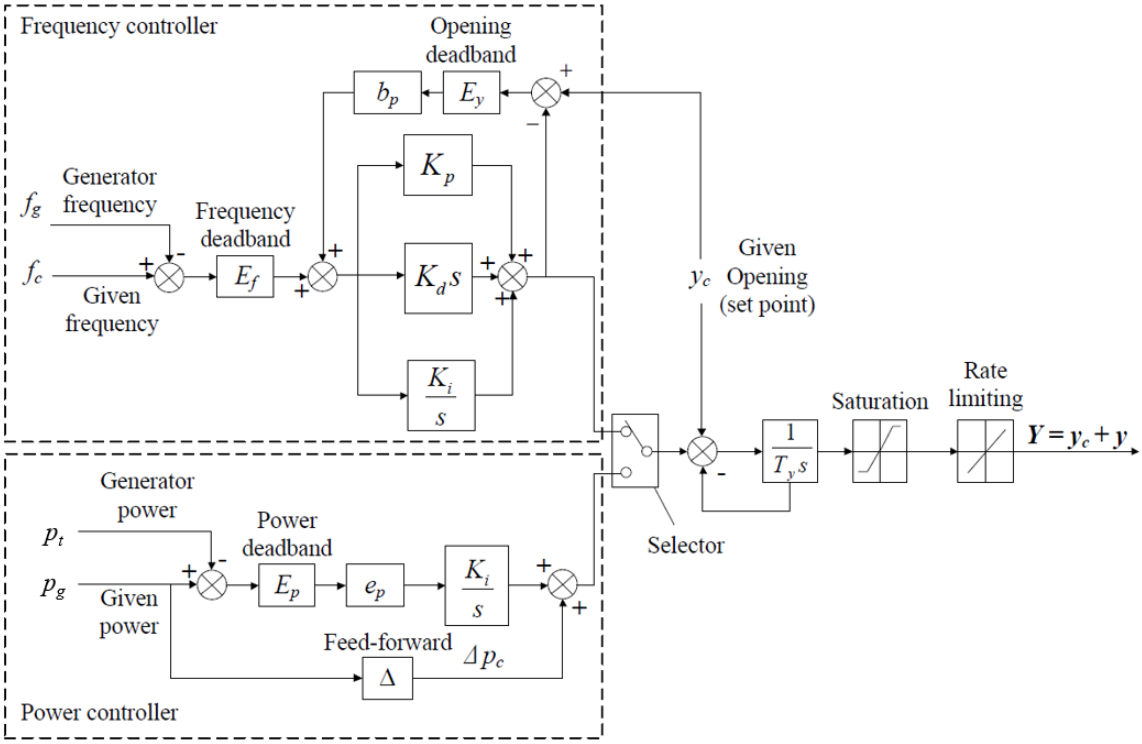

Figure 3. Diagram of governor with switch-over function of control mode

$$b_p K_d T_y \frac{d^3 y}{dt^3} + (T_y + b_p K_p T_y + K_d K_p) \frac{d^2 y}{dt^2} + (1 + b_p K_p + b_p K_i T_y) \frac{dy}{dt} + b_p K_i y = -(K_d \frac{d^2 x}{dt^2} + K_p \frac{dx}{dt} + K_i x) \quad (8)$$

The governor, with a selector of the PID frequency controller and the "integral + feed-forward" power controller, is shown in Figure 3. The final value of guide vane opening (Y) is the sum of set point (y_c) and deviation (y). The differential equation of

frequency control is shown in Eq. (8), more exactly, Eq. (8) is equivalent with Eq. (6) when the value of K_d is set 0. The differential equation of power control is the same as Eq. (7). Besides, the dead-band, saturation and rate limiting are contained in the model. Their effect can be reflected in simulations, but they are omitted in the equations because of their nonlinear nature.

2.3 Engineering case

The engineering case, for both theoretical derivation and numerical simulation, is a huge Chinese HPP with an upstream surge tank, huge power output and long draw water tunnel. Details of the engineering case are found in Appendix B. A model of this HPP is built by applying the extended software TOPSYS, as shown in Figure 4.

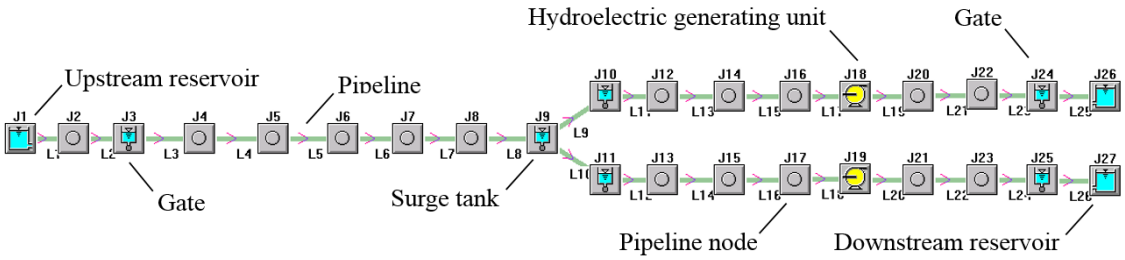

Figure 4. Model of the HPP built by extended software TOPSYS

3 Theoretical derivation with Hurwitz criterion

3.1 Stability condition

Stability condition of frequency oscillation under frequency control and power control is obtained by adopting Hurwitz criterion.

145 3.1.1 Frequency control

146 By applying the Laplace transform to Eqs. (1-6), the transfer function of hydraulic-

147 regulating system is obtained:

$$G(s)=\frac{X(s)}{M_g(s)}=-\frac{(1+T_F ms+me_{qh})\left[T_y(1+b_pK_p)s^2+(1+b_pK_p+b_pK_iT_y)s+b_pK_i\right]}{a_0s^5+a_1s^4+a_2s^3+a_3s^2+a_4s+a_5} \tag{9}$$

148 The fifth-order differential motion equation of frequency control is derived from the

149 transfer function:

$$a_0\frac{d^5x}{dt^5}+a_1\frac{d^4x}{dt^4}+a_2\frac{d^3x}{dt^3}+a_3\frac{d^2x}{dt^2}+a_4\frac{dx}{dt}+a_5x=0 \tag{10}$$

150 The details of the symbols in the equations above are given in Appendix C.

151 For frequency control, the stability condition is:

$$\Delta_1=a_i>0\ (\ i=0,\ 1,\ 2,\ 3,\ 4,\ 5) \tag{11}$$

$$\Delta_2=a_1a_2-a_0a_3>0 \tag{12}$$

$$\Delta_4=(a_1a_2-a_0a_3)(a_3a_4-a_2a_5)-(a_1a_4-a_0a_5)^2>0 \tag{13}$$

152

153 3.1.2 Power control

154 In the equation of power control, the ordinary expression of p_t is $p_t = m_tx + m_t + x$, but

155 m_t and x are micro for small load disturbance. In order to maintain linearity of equation,

156 the expression of p_t can be simplified to $p_t = m_t + x$ by ignoring the second-order term

157 m_tx. Therefore Eq. (7) is transferred to Eq. (14) from Eq. (5) and the simplified

158 expression of p_t:

$$T_y\frac{\mathrm{d}^2y}{\mathrm{d}t^2}+\frac{\mathrm{d}y}{\mathrm{d}t}=-e_pK_IT_a\frac{\mathrm{d}x}{\mathrm{d}t}-e_pK_I(e_g+1)x \tag{14}$$

159 The fifth-order differential equation of motion of power control is derived from Eqs.

(1-5) and Eq. (14):

$$a_0' \frac{d^5x}{dt^5} + a_1' \frac{d^4x}{dt^4} + a_2' \frac{d^3x}{dt^3} + a_3' \frac{d^2x}{dt^2} + a_4' \frac{dx}{dt} + a_5' x = 0 \quad (15)$$

The details of the symbols in the equations above are given in Appendix C.

The differential equations of motion of two control modes are both fifth-order. Therefore, the stability condition of power control is the same as which of frequency control by replacing the a_i to a_i' in Eqs. (11-13).

3.2 Stability analysis of two control modes

This section makes contrast and analysis of stability regions of two control modes based on the engineering case. The stability region is the region which satisfies the stability condition in K_i-n coordinates by substituting the system parameters of different states into the stability condition. The value n ($n = F/F_{th}$) stands for the coefficient of cross section area of surge tank, F and F_{th} are the real area and Thoma critical area [2], respectively. In terms of the drawing method of stability region, firstly, curves which correspond to critical stability condition are drawn in K_i-n coordinates, and then the envelope of curves is obtained. The envelope is the boundary of stability region and the right portion is the stability region.

The related parameter values are given in Appendix B. Based on the stability condition, a set of curves of stability region boundaries is achieved under two control modes, as shown in Figure 5. The stability region of power control is much larger than which of frequency control. There is no proportional gain (K_p can be regarded as 0) in

power control, and it is conducive to the stability. However under frequency control, when the K_p is set to near 0, the stability region is still smaller than for power control. Besides, the head loss and the ratio T_w/T_a also affect the stability, and they should be further discussed. In conclusion, from the theoretical derivation, it is found that the stability performance under power control is better than which is under frequency control.

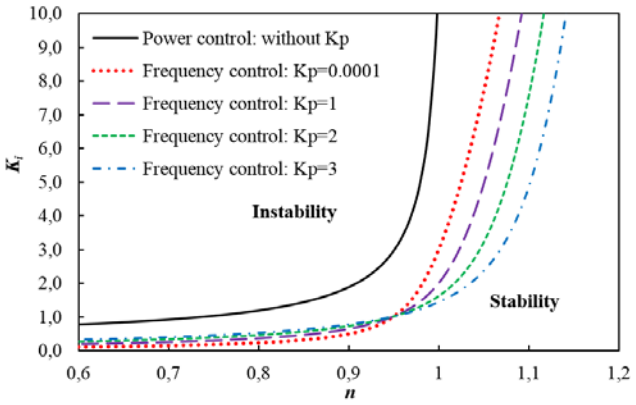

Figure 5. Stability region in K_i-n coordinates of two control modes

4. Numerical simulation

In the section, numerical simulation is applied to validate the result of theoretical derivation, and to explore the worst operation cases and solutions of frequency unsteadiness. Idealized cases, which are the load step disturbances (610MW decrease to 549MW), are simulated under two control modes.

4.1 Stability under two control modes with different governor parameters

In the simulation, different values of K_p and K_i are adopted, and other parameters are set

197 to the same values as in section 3, see Appendix B. Results are shown in Figure 6 and
198 Figure 7.

199 From the simulation, the conclusion drawn in section 3 is verified: the power
200 control produces a better effect on stability than frequency control. More specifically,
201 under frequency control, it is hard to stabilize the frequency by adopting any of the three
202 sets of parameters. Even when K_p is set to nearly 0, to compare with the power
203 controller which is without proportion component (K_p = 0), the frequency instability still
204 occurs. With the decrease of the governor parameter, the frequency has a tendency to
205 stabilize, whereas the rapidity becomes worse. Hence, the governor parameters should
206 be tuned to ensure the stability and rapidity simultaneously. While under power control,
207 frequency stability is well ensured, and the contradiction between rapidity and stability
208 is also indicated.

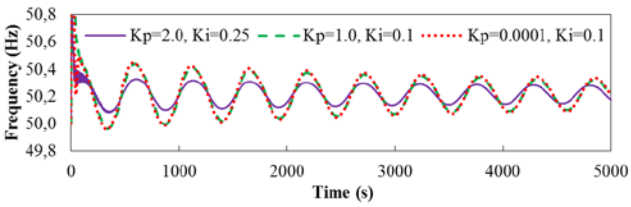

Figure 6. Frequency oscillation under frequency control with different governor parameters

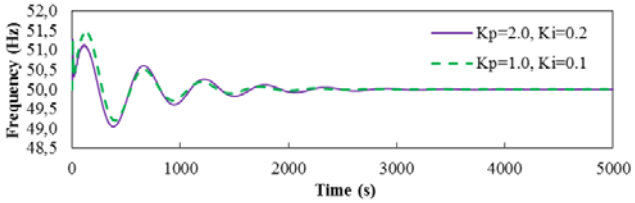

Figure 7. Frequency oscillation under power control with different governor parameters

209 It is worth noting that the instability usually refers to the oscillation with increasing
210 amplitude, however in this practical study, a stable oscillation is also regarded as
211 instability. Besides, the steady-state frequency error, due to the permanent speed droop
212 (b_p), occurs after a load disturbance under frequency control (primary control), and it

could be corrected by secondary control. However the frequency error is not discussed in this paper, only the stability performance is the main concern.

4.2 Stability under two control modes with different operation case

The water inertia of water way system is adverse to regulating stability [21]. However, former research make the analysis of water inertia time constant ($T_w = \frac{Q}{gH}\sum\frac{L}{f}$) just from the view of layout and design of HPP by focusing on length (L) and section area (f) of piping, while the discharge (Q) and water head (H) are seldom studied. Therefore in this section, different operation cases, with different loads and operating water levels, are analyzed under two control modes, as shown in Table 1, Figure 8 and Figure 9. Moreover, for six cases in Table 1, the upsteam water levels are 1640.0 m and "final state" means the steady state after the load disturbance whereas the discharge and water head are obtained by calculation of steady flow. Besides, the governor parameters are the same under two control modes (recommended value): K_p = 2.0, K_i = 0.25, other parameters are shown in Appendix B.

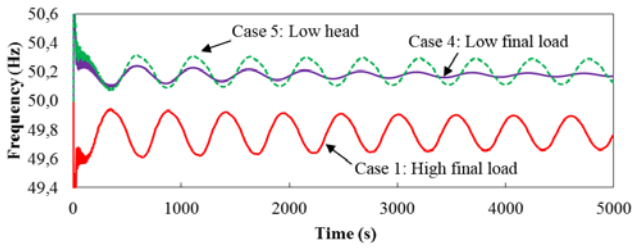

Figure 8. Influence of final state and operating water level (frequency control)

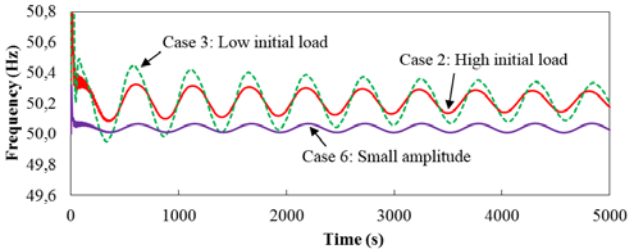

Figure 9. Influence of initial state and amplitude of load disturbance (frequency control)

Table 1. Related parameters of HPP operation case

Case	Downstream water level (m)	Load step disturbance	Water head of final state (m)	Discharge of final state (m^3/s)	Q/H (m^2/s)
1	1331.94	90%-100%	292.96	224.19	0.765
2	1331.94	100%-90%	296.53	197.32	0.665
3	1331.94	80%-90%	296.53	197.32	0.665
4	1331.94	90%-80%	299.24	172.73	0.577
5	**1341.94**	90%-80%	288.60	178.81	0.620
6	1331.94	**92%-90%**	296.53	197.32	0.665

For frequency control, according to Figure 8 and Figure 9, under unfavorable cases, the instability phenomenon is obviously reflected by the constant amplitude of frequency oscillation. Under different cases, the initial load has no effect on the frequency stability (the contrast between case 2 and case 3 in **Figure** 9). In contrast, large load of final state (the contrast between case 1 and case 4 in Figure 8) or low water head (the contrast between case 4 and case 5 in Figure 8) results in large water inertia of final state (indicated by the value of Q/H in Table 1) and goes against the frequency stability. The load disturbance amplitude has little influence on frequency stability, but it determines the amplitude of frequency oscillation, see case 6. In summary, under frequency control, the HPP shows poor frequency stability, and the worst operation case is when the load ascends from 90% to 100% of rated power under the lowest water head.

The simulation under power control is described in Figure 10 and Figure 11. The power control has an obviously better effect on stability which is influenced only little by diverse operation cases. Even for the worst case of frequency control, the stability is still guaranteed. By contrast, the regulation rapidity cannot be ensured well. It is takes a few periods for frequency oscillation amplitude to decay to an acceptable range, and the

larger amplitude of load disturbance, the longer setting time.

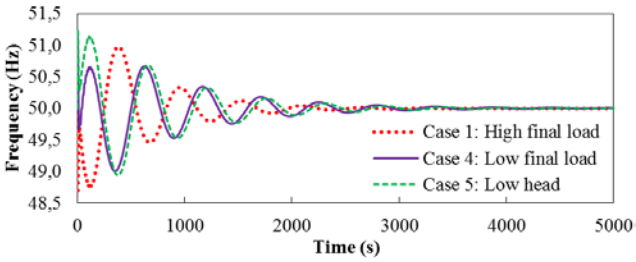

Figure 10. Influence of final state and operating water level (power control)

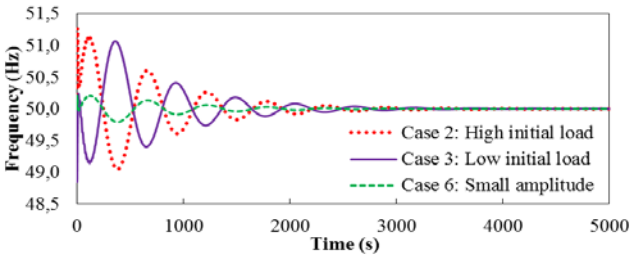

Figure 11. Influence of initial state and amplitude of load disturbance (power control)

For operation cases with small water inertia of final state, it is appropriate to adopt frequency control to ensure the stability and rapidity simultaneously. Otherwise, the power control could be applied to guarantee the stability at the expense of rapidity.

4.3 Frequency oscillation under control mode switch-over

If the instability already occurs under frequency control, could the stability be re-obtained by manually switching the control mode to power control? In this section, this case is simulated to investigate the frequency oscillation during the control mode switch-over.

The simulation of the control mode switch-over is shown in Figure 12, for the case 2 in Table 1. In order to compare the results clearly, the steady-state frequency error is diminished by setting the droop b_p to 0. The control mode is manually converted to power control at 1200 s, when the frequency oscillation tends to be unstable under frequency control. The frequency oscillation amplitude increases immediately under the influence of water level fluctuation in surge tank, because of the relatively poor rapidity

of power control, and afterwards it takes several periods for the frequency oscillation to stabilize again. In short, the stability could be re-obtained finally by control mode switch-over, although the frequency oscillation amplitude would increase during the transient process. Therefore the control mode switch-over is a simple and effective option for re-obtaining the frequency stability.

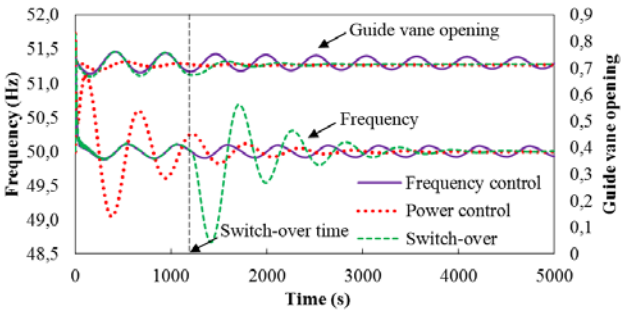

Figure 12. Oscillation of frequency and guide vane opening under control mode switch-over

5 Conclusions

In this study, a theoretical model, containing the governor equations of frequency control and power control, and a simulation model with control mode switch-over function are built. Frequency stability under power control is investigated and compared to frequency control, with various operation cases.

The conclusions are drawn as follows: (1) the power control has a better performance on frequency stability, comparing with the frequency control. By contrast, power control leads to poorer rapidity. (2) The water inertia of final state is a key factor of frequency stability. The worst operation case for stability is with large load, large load disturbance amplitude and low water head of final state. So a suggested case of

isolated operation, for simulation or test, to exam the stability could be: load (or power output) ascends from 90% to 100% of rated power under the lowest water head. (3) For the operation case with small water inertia of final state, it is appropriate to adopt frequency control to ensure the stability and rapidity simultaneously. Otherwise, the power control can be applied to guarantee the stability at the expense of rapidity. Besides, the simulaion also shows that if the instability already occurs under frequency control, the stability could be re-obtained by manually switching the control mode to power control, although the frequency oscillation amplitude would increase temporarily during the switch-over transient process.

This study lays a foundation for the future research on stability of islanded or interconnected operation of multiple power-generating units or HPPs, for example a study on optimizing the combination of units in different control modes to enhance the whole system stability.

Acknowledgements

The authors acknowledge the support from the National Natural Science Foundation of China under Grant No. 51039005 and Grant No. 51379158. The authors also thank the China Scholarship Council (CSC), StandUp for Energy. The research presented was also carried out as a part of "Swedish Hydropower Centre - SVC". SVC has been established by the Swedish Energy Agency, Elforsk and Svenska Kraftnät together with Luleå University of Technology, KTH Royal Institute of Technology, Chalmers University of

300 Technology and Uppsala University. www.svc.nu.

301

302 **Appendix A. List of symbols**

303 $q_y = \frac{Q_y - Q_{y0}}{Q_{y0}}$ discharge of draw water tunnel

304 $q_t = \frac{Q - Q_0}{Q_0}$ discharge of turbine

305 $x = \frac{n_t - n_0}{n_0} = \frac{f_g - f_c}{f_c}$ rotation speed of turbine

306 $y = \frac{Y - Y_0}{Y_0}$ guide vane opening

307 $m_t = \frac{M_t - M_{t0}}{M_{t0}}$ dynamic moment of turbine

308 $m_g = \frac{M_g - M_{g0}}{M_{g0}}$ braking moment of generator

309 $p_t = \frac{P_t - P_{t0}}{P_{t0}}$ power of hydroelectric generating unit

310 $p_g = \frac{P_g - P_{g0}}{P_{g0}}$ given power of hydroelectric generating unit

311 $z = \frac{\Delta Z}{H_0}$ relative change value of water level in surge tank

312 Symbols above are all relative values (per unit values), and symbols with subscript “0”

313 stands for initial value.

314

315 $\triangle Z$ absolute change value of water level in surge tank

316 H_0 net head of turbine

317 h_{yo} head loss of draw water tunnal

318 T_{wy} water inertia time constant of draw water tunnel

$T_F = \frac{FH_0}{Q_{y0}}$	surge tank time constant
F	cross section area of surge tank
T_a	generating unit inertia time constant
e_h, e_x, e_y	moment transmission coefficient of turbine
e_{qh}, e_{qx}, e_{qy}	discharge transmission coefficient of turbine
e_g	characteristic coefficient of power grid load
K_p, K_i, K_d, T_y, b_p, e_p	governor parameters which are shown in Figure 3

Appendix B. Details of the engineering case

Rated power of generating unit: 610 MW

Rated water head of generating unit: 288.0 m

Rated discharge of generating unit: 228.6 m^3/s

Rated rotation speed of generating unit: 166.7 r/min

Length of draw water tunnel: 16662.16 m

T_{wy} of draw water tunnel: 23.88 s

T_w of penstock: 1.35 s

Head loss: 15.67 m

Equivalent section area of draw water tunnel: 113.10 m^2

Inertia time constant of generating unit (T_a): 9.46 s

Length of penstock: 513.34 m

Other governor parameters: K_d = 0, T_y = 0.02, b_p = 0.04, e_p = 0.04, E_f = E_y =E_p= 0

Characteristic coefficient of power grid load: e_g = 0.0

Transmission coefficient of ideal turbine: e_h = 1.5, e_x = -1,e_y = 1, e_{qh} = 0.5, e_{qx} = 0, e_{qy} = 1

Cross section area of surge tank (F): 415.64 m^2

Thoma critical section area for stability (F_{th}): 416.08 m^2

Appendix C. Symbols in Section 3.1

(1) Symbols in Eqs. (9-10): frequency control

$$m = T_{wy}s + \frac{2h_{y0}}{H_0},\ a_0 = f_4 T_y (1 + b_P K_P),\ a_1 = f_5 T_y (1 + b_P K_P) + f_4 (1 + b_P K_P + b_P K_I T_y)$$

$$a_2 = f_6 T_y (1 + b_P K_P) + f_5 (1 + b_P K_P + b_P K_I T_y) + f_4 b_P K_I + f_1 K_P$$

$$a_3 = f_7 T_y (1 + b_P K_P) + f_6 (1 + b_P K_P + b_P K_I T_y) + f_5 b_P K_I + f_2 K_P + f_1$$

$$a_4 = f_7 (1 + b_P K_P + b_P K_I T_y) + f_6 b_P K_I + f_3 K_P + f_2 K_I,\ a_5 = f_7 b_P K_I + f_3 K_I$$

$$f_1 = e_y T_F T_{wy},\ f_2 = e_y (e_{qh} T_{wy} + T_F \frac{2h_{y0}}{H_0}) - e_h e_{qy} T_{wy},\ f_3 = e_y (1 + e_{qh} \frac{2h_{y0}}{H_0}) - e_h e_{qy} \frac{2h_{y0}}{H_0},\ f_4 = T_a T_F T_{wy},$$

$$f_5 = T_F T_{wy} (e_g - e_x) + T_a (T_F \frac{2h_{y0}}{H_0} + T_{wy} e_{qh}) \quad , \quad f_6 = (e_g - e_x)(T_F \frac{2h_{y0}}{H_0} + T_{wy} e_{qh}) + T_a (1 + e_{qh} \frac{2h_{y0}}{H_0}) + e_h e_{qx} T_{wy} \quad ,$$

$$f_7 = (e_g - e_x)(1 + e_{qh} \frac{2h_{y0}}{H_0}) + e_h e_{qx} \frac{2h_{y0}}{H_0}$$

(2) Symbols in Eq. (15): power control

$$a_0' = T_{wy} T_F T_y T_a,\ \ a_1' = T_{wy} T_F T_y b_2 + T_y T_a b_0 + T_{wy} T_F T_a$$

$$a_2' = T_y b_0 b_2 + T_y T_a b_1 + T_{wy} T_y e_h e_{qx} + T_{wy} T_F b_2 + T_a b_0 + e_y T_{wy} T_F b_4$$

$$a_3' = T_y b_1 b_2 + T_y e_{qx} b_3 + b_0 b_2 + T_a b_1 + T_{wy} e_h e_{qx} + (e_y b_0 - T_{wy} e_h e_{qy}) b_4 + e_y T_{wy} T_F b_5$$

$$a_4' = b_1 b_2 + e_{qx} b_3 + (e_y b_0 - T_{wy} e_h e_{qy}) b_5 + (e_y b_1 - e_{qy} b_3) b_4,\ a_5' = (e_y b_1 - e_{qy} b_3) b_5,$$

$$b_0 = \frac{2h_{y0} T_F}{H_0} + T_{wy} e_{qh},\ b_1 = \frac{2h_{y0} e_{qh}}{H_0} + 1,\ b_2 = e_g - e_x,\ b_3 = \frac{2h_{y0} e_h}{H_0},\ b_4 = e_p K_I T_a,\ b_5 = e_p K_I (e_g + 1)$$

References

[1] Kundur P, Paserba J, Ajjarapu V, Andersson G, Bose A, Canizares C, et al. "Definition and classification of power system stability," *Ieee T Power Syst*. Vol. 19, No. 3, pp. 1387-1401, 2004.

[2] Jaeger C. Fluid transients in hydro-electric engineering practice: Blackie; 1977.

[3] Krivchenko GI. "Admissibility of deviating from the Thoma criterion when designating the cross-sectional area of surge tanks," *Hydrotechnical Construction*. Vol. 22, No. 7, pp. 403-409, 1988.

[4] Liang F, Jiandong Y, Haiyan B, Jinping L. "Effect of Turbine Characteristic on the Response of Hydroturbine Governing System with Surge Tank," *Power and Energy Engineering Conference, 2009 APPEEC 2009 Asia-Pacific*. 1-6, 2009.

[5] Murav'ev OA, Berlin VV. "Operating stability of hydroelectric stations with downstream surge tanks," *Hydrotechnical Construction*. Vol. 29, No. 4, pp. 242-247, 1995.

[6] Yang L. "The extending application of Ляпунов′s Stability Theory in the subject of water level oscillating stability in the surge tank [In Chinese]," *Journal of Hydraulic Engineering*. Vol. 30, No. 9, pp. 33-37, 1999.

[7] Doolla S, Bhatti TS, Bansal RC. "Load Frequency Control of an Isolated Small Hydro Power Plant Using Multi-pipe Scheme," *Elect Power Compon Syst*. Vol. 39, No. pp. 46–63, 2011.

[8] Vournas CD, Papaioannou G. "Modelling and stability of a hydro plant with two surge tanks," *Energy Conversion, IEEE Transactions on*. Vol. 10, No. 2, pp. 368-375, 1995.

[9] Zoby MRG, Yanagihara JI. "Analysis of the Primary Control System of a Hydropower Plant in Isolated Model," *J Braz Soc Mech Sci*. Vol. 31, No. 1, pp. 5-11, 2009.

[10] Hannett LN, Feltes JW, Fardanesh B, Crean W. "Modeling and control tuning of a hydro station with units sharing a common penstock section," *Power Systems, IEEE Transactions on*. Vol. 14, No. 4, pp. 1407-1414, 1999.

[11] Mansoor SP, Jones DI, Bradley DA, Aris FC, Jones GR. "Stability of a pump storage hydro-power station connected to a power system," *Ieee Power Engineering Society - 1999 Winter Meeting, Vols 1 and 2*. Vol., No. pp. 646-650, 1999.

[12] Landry C, Nicolet C, Giacomini S, Avellan F. Influence of the Hydraulic System Layout on the Stability of a Mixed Islanded Power Network, Advances in Hydroinformatics: Springer Singapore; 2014. pp. 307-323.

[13] Liu XL, Liu C. "Eigenanalysis of oscillatory instability of a hydropower plant including water conduit dynamics," *Ieee T Power Syst*. Vol. 22, No. 2, pp. 675-681, 2007.

[14] Nicolet C, Greiveldinger B, Herou JJ, Kawkabani B, Allenbach P, Simond JJ. "High-order modeling of hydraulic power plant in islanded power network," *Ieee T Power Syst*. Vol. 22, No. 4, pp. 1870-1880, 2007.

[15] Murty MSR, Hariharan MV. "Analysis and Improvement of the Stability of a Hydro-Turbine Generating-Unit with Long Penstock," *Ieee T Power Ap Syst*. Vol. 103, No. 2, pp. 360-367, 1984.

[16] Mansoor SP, Jones DI, Bradley DA, Aris FC, Jones GR. "Reproducing oscillatory behaviour of a hydroelectric power station by computer simulation," *Control Eng Pract*. Vol. 8, No. 11, pp. 1261-1272, 2000.

[17] Pico HV, McCalley JD, Angel A, Leon R, Castrillon NJ. "Analysis of Very Low Frequency Oscillations in Hydro-Dominant Power Systems Using Multi-Unit Modeling," *IEEE Trans Power Sys*.

Vol. 27, No. 4, pp. 1906-1915, 2012.

[18] Bao HY, Yang JD, Fu L. "Study on Nonlinear Dynamical Model and Control Strategy of Transient Process in Hydropower Station with Francis turbine," *Asia-Pac Power Energ*. Vol., No. pp. 165-170, 2009.

[19] IEC. "Guide to specification of hydraulic turbine control systems." 1998.

[20] "IEEE Guide for the Application of Turbine Governing Systems for Hydroelectric Generating Units," *IEEE Std 1207-2004*. 2004.

[21] Lai X, Yang J, Chen J. "The Effect of Sectional Area of Surge Tank on Stability of Turbine Regulation System [In Chinese]," *Engineering Journal of Wuhan University*. Vol. 30, No. 4, pp. 13-17, 1997.